Journal of Soils and Sediments (2018) 18:1668–1678
https://doi.org/10.1007/s11368-017-1883-1

SOILS, SEC 5 • SOIL AND LANDSCAPE ECOLOGY • RESEARCH ARTICLE

Fe(II) oxidation and nitrate reduction by a denitrifying bacterium, *Pseudomonas stutzeri* LS-2, isolated from paddy soil

Shuang Li[1,2,3] · Xiaomin Li[2] · Fangbai Li[2]

Received: 29 June 2017 / Accepted: 24 November 2017 / Published online: 1 December 2017

Abstract

Purpose Ferrous iron (Fe(II)) oxidation and nitrate (NO_3^-) reduction are commonly observed in environments with denitrifying bacteria. The intermediate nitrite (NO_2^-) from denitrification can chemically oxidize Fe(II). However, it is difficult to distinguish how chemical and biological reactions are involved. *Pseudomonas stutzeri* LS-2, a denitrifying bacterium isolated from paddy soil in southern China, was used in this study to investigate the chemical and biological reactions contributing to Fe(II) oxidation and NO_3^- reduction under denitrifying conditions.

Materials and methods Concentrations of dissolved Fe(II), NO_3^-, NO_2^-, and nitrous oxide (N_2O) over time were quantified to investigate the kinetics of Fe(II) oxidation and NO_3^-/NO_2^- reduction in different treatments (i.e., microbial treatments: Cell + NO_3^- and Cell + NO_2^-, chemical treatment: Fe(II) + NO_2^-, and combined treatments: LS-2 + Fe(II) + NO_3^- and LS-2 + Fe(II) + NO_2^-). Stable isotope fractionations of $\delta^{15}N$-N_2O in different treatments were also determined over time. Fe(III) minerals and cell-mineral precipitates formed due to Fe(II) oxidation after 6 days of incubation were characterized using X-ray diffraction (XRD), scanning electron microscopy (SEM), and transmission electron microscopy (TEM).

Results and discussion *P. stutzeri* LS-2 could completely reduce NO_3^- or NO_2^- within 2 days in the microbial treatment of Cell + NO_3^- or Cell + NO_2^-. The presence of Fe(II) resulted in a decrease of NO_3^- or NO_2^- reduction rates and an increase in the amount of nitrous oxide (N_2O) production in the combined treatments of Cell + Fe(II) + NO_3^- and Cell + Fe(II) + NO_2^-. Fe(II) oxidation was only observed in the two combined treatments and the chemical treatment of Fe(II) + NO_2^-. Lepidocrocite was formed due to Fe(II) oxidation after 6 days of incubation, which fully covered the bacterial cell surfaces in both combined treatments. Encrustation occurred in the periplasm and on the cell surface. The $\delta^{15}N$-N_2O were 7.8 to − 10‰ in both microbial treatments during incubation, while those were − 23 to − 15‰ in the Fe(II) + NO_2^- and Cell + Fe(II) + NO_2^- treatments. In the Cell + Fe(II) + NO_3^- treatment, however, the $\delta^{15}N$ in N_2O were − 37 to − 25‰, which were different from the microbial and chemical treatments. This difference is probably due to the accelerated reaction between Fe(II) and NO_3^-/NO_2^- by lepidocrocite.

Conclusions Our results indicate that once NO_3^- was reduced to NO_2^- by the denitrifying bacterium *P. stutzeri* LS-2, the NO_2^- chemically reacted with Fe(II), and the concomitant Fe(III) oxide formation and cell encrustation led to an inhibition to denitrification. The stable isotope fractionation technique in combination with the transformation kinetics analyses is useful to distinguish the chemical and biological reactions involved in Fe(II) oxidation and nitrate reduction by denitrifying bacteria.

Keywords Nitrate reduction · Fe(II) oxidation · Denitrifying bacterium · Nitrogen isotope fractionation · Microbial and chemical reactions

Responsible editor: Jizheng He

Electronic supplementary material The online version of this article (https://doi.org/10.1007/s11368-017-1883-1) contains supplementary material, which is available to authorized users.

✉ Xiaomin Li
xmli@soil.gd.cn

[1] Guangzhou Institute of Geochemistry, Chinese Academy of Sciences, Guangzhou 510640, China

[2] Guangdong Key Laboratory of Agricultural Environment Pollution Integrated Control, Guangdong Institute of Eco-Environmental Science and Technology, Guangzhou 510650, China

[3] Graduate University of The Chinese Academy of Sciences, Beijing 100039, China

1 Introduction

Denitrification is an important microbial process in which nitrate (NO_3^-) undergoes dissimilatory reduction to nitrogen gas (N_2) in the following sequential reactions: $NO_3^- \rightarrow$

$NO_2^- \rightarrow NO \rightarrow N_2O \rightarrow N_2$ (Xu and Enfors 1996). Most denitrifying microorganisms are aerobic heterotrophic organisms that transfer redox equivalents from the oxidation of a carbon source to an N oxide under anoxic conditions (Zumft 1997). As the oxidation of ferrous iron (Fe(II)) is coupled to the denitrification process (Straub et al. 1996), this phenomenon has been discovered in various habitats, such as freshwater sediments, costal marine sediments, and paddy soils (Muehe et al. 2009; Laufer et al. 2015; Li et al. 2016). The interaction between denitrification and Fe(II) oxidation not only affects the biogeochemistry transformation of nitrogen and iron (Mejia et al. 2016; Wang et al. 2016) but also influences the fate of other elements, such as carbon and heavy metals (Yu et al. 2017).

Several bacteria have been reported to couple nitrate reduction and Fe(II) oxidation in pure cultures, such as *Pseudogulbenkiania* sp. (Weber et al. 2006) and *Acidovorax* sp. (Kappler et al. 2005; Byrne-bailey et al. 2010; Chakraborty et al. 2011). There is evidence that the capacity for nitrate-reducing Fe(II) oxidation is widespread and likely innate to the denitrifying bacteria, such as *Paracoccus denitrificans* and *Pseudomonas stutzeri* (Muehe et al. 2009; Klueglein et al. 2014). The intermediate nitrite (NO_2^-) in the denitrification pathway can chemically oxidize Fe(II) (chemodenitrification), producing nitric oxide (NO) and nitrous oxide (N_2O) gases along with Fe(III) (hydr)oxides as byproducts (Carlson et al. 2013; Melton et al. 2014). However, the contribution of the microbial and chemical reactions in the observed nitrate-reducing Fe(II) oxidation remains unclear. As the number of denitrifying bacteria in the environment is significantly higher than that of nitrate-reducing Fe(II) oxidizers (Straub and Buchholz-cleven 1998; Muehe et al. 2009), it is important to investigate how microbial and chemical reactions are involved in nitrate reduction and Fe(II) oxidation under denitrifying conditions.

Stable isotope analysis of N_2O (particularly the ^{15}N–isotopomer) can be useful to disentangle the different pathways leading to N_2O formation in natural environments and pure cultures (Toyoda et al. 2005; Sutka et al. 2006; Heil et al. 2014). Regarding the microbial pathways, the different isotopic compositions of N_2O in the denitrification and nitrification processes have been used to evaluate their relative contribution in N_2O production (Sutka et al. 2006; Wunderlin et al. 2012). For chemical pathways, the characteristic isotopic composition of N_2O involved in chemodenitrification has been recently reported (Jones et al. 2015). The $\delta^{15}N$ values of N_2O were utilized to distinguish between chemical and biological reduction of NO_2^- by an iron-reducing bacterium in which the N_2O produced during NO_3^- reduction in the presence of goethite was primarily of abiotic origin (Cooper et al. 2003). In this study, the $\delta^{15}N$ in N_2O was characterized to determine the N_2O origin during Fe(II) oxidation and nitrate reduction by denitrifying bacteria.

A variety of Fe(III) (hydr)oxide minerals can be formed during nitrate-reducing Fe(II) oxidation, including ferrihydrite (Lack et al. 2002), goethite (Senko et al. 2005), lepidocrocite (Larese-Casanova et al. 2010), magnetite (Chaudhuri et al. 2001), green rust (Chaudhuri et al. 2001), and vivianite (Miot et al. 2009). The Fe(III) mineral type is strongly dependent on the geochemical solution conditions, such as carbonate, phosphate, pH, and humic acids (Larese-Casanova et al. 2010). Formation of green rust as an intermediate mineral (followed by goethite formation as final Fe(III) product) and cell encrustation have been characterized due to abiotic Fe(II) oxidation by NO_2^- from heterotrophic denitrification (Nordhoff et al. 2017). Chemodenitrification can also produce ferrihydrite, lepidocrocite, and goethite which, in combination with the characteristic isotopic fractionation, is proposed to be useful to distinguish qualitatively between microbially and chemically emitted N_2O (Jones et al. 2015).

In this study, a denitrifying bacterium, *Pseudomonas stutzeri* LS-2, isolated from red paddy soil in southern China was used to investigate the kinetics of nitrate reduction and Fe(II) oxidation under denitrifying conditions. Stable isotope fractionation of $\delta^{15}N$-N_2O, as well as Fe(III) mineral formation, was characterized to clarify how chemical and biological reactions were involved in the NO_3^- reduction and Fe(II) oxidation mediated by *P. stutzeri* LS-2.

2 Materials and methods

2.1 Soil sampling and isolation of the strain

P. stutzeri strain LS-2 was isolated from paddy soil in Shantou City, Guangdong Province, China (23° 38′ 30.4″ N, 116° 50′ 4.7″ E). The geochemical properties of the paddy soil are as follows: pH 7.3, organic matter: 13.1 g kg^{-1}, total As: 0.301 g kg^{-1}, total Fe: 30.5 g kg^{-1}, DCB-extractable (dithionite-citrate-bicarbonate) Fe: 17.3 g kg^{-1}, amorphous Fe: 0.403 g kg^{-1}. The soil sample was collected 10–20 cm below the soil surface and stored in an anaerobic sterile-sealed container. Upon arrival to the laboratory, the soil sample was cultured in 100-mL sterilized sealed bottles with butyl rubber stoppers containing sterile denitrifier basal medium (DBM) with a ratio of soil to DBM at 1:10 for enrichment. The bottle headspaces were filled with N_2 and the enrichment cultures were incubated in an anaerobic workstation at 30 ± 1 °C in the dark. By regular subculturing at 7-day intervals, 10% (*v*/*v*) inoculum was transferred to fresh DBM medium. The enriched populations were serially diluted and streaked on the DBM agar plates for isolation. Distinct colonies were picked and tested in the DBM medium to confirm their ability to reduce NO_3^-. The DBM medium contained 30 mM PIPES [piperazine-N, N`-bis (2-ethanesulfonic acid)] buffer (pH 7.0 ± 0.2), 10 mM $NaNO_3$, 5 mM sodium acetate, and

1 mL L^{-1} each of the trace element solution and vitamin solution (Bruce et al. 1999). The trace element and vitamin solutions were filtered using a 0.22 μm filter and other medium was autoclaved at 120 °C for 25 min before use.

The genomic DNA of the strain was extracted using the EZNA™ Bacterial DNA Kit (Omega Bio-Tek, Inc., Norcross, GA, USA) after the manufacturer's instructions. The 16S rRNA gene was amplified by PCR using universal bacterial primers (27F, 5-AGAGTTTGATCCTGGCTCAG-3 and 1492R, 5-GGTTACCTTGTTACGACTT-3) as described by Delong (1992). The amplified PCR product was tested by gel electrophoresis and purified using a DNA Gel Extraction Kit (Omega Bio-Tek, Inc., Norcross, GA, USA). The purified PCR product was cloned using the pGEM-T Vector System (Promega, Madison, WI) and transformed into *E. coli* JM109 competent cells. Positive clones were selected randomly and sequenced by Sangon Biotech (Shanghai, China). The sequences were searched against the GenBank database (http://blast.ncbi.nlm.nih.gov/) to determine the closest matches using the BLAST program. A phylogenetic tree was constructed by using the neighbor-joining (NJ) algorithm in the MEGA 6.0 program.

2.2 Fe(II) oxidation and nitrate/nitrite reduction experiments

The isolated strain was cultured in LB medium for 12 h in a shaker at 180 rpm and 30 °C. The LB medium contained (g L^{-1}): tryptone, 10; yeast extract, 5; NaCl, 10; pH 7.0 ± 0.2. The strain was harvested by centrifugation at 10,000 rpm for 10 min at 4 °C following being washed and re-suspended with sterile and anoxic PIPES buffer (30 mM, pH 7.0 ± 0.2) for three times. A total of seven treatments were conducted, and the details are presented in Table 1. The initial concentrations of $FeCl_2{\cdot}4H_2O$, $NaNO_3$, $NaNO_2$, and acetate were 5, 10, 4, and 5 mM, respectively. The cell density was approximately 3.8×10^8 cells mL^{-1}. PIPES buffer (30 mM) was added to maintain the pH at 7.0 ± 0.2. The serum bottles were purged with N_2 for 30 min, sealed with butyl rubber stoppers and aluminum crimp seals, and incubated at 30 ± 1 °C in the anaerobic workstation in the dark. NO_3^-, NO_2^-, N_2O, and Fe(II) concentrations were measured at intervals. The kinetics constants of Fe(II) oxidation and NO_3^-/NO_2^- reduction were calculated based on the first-order reaction formulas $k_t = \ln(C_0/C_t)$.

2.3 Measurements of nitrate, nitrite, N_2O, Fe(II)

To determine NO_3^- and NO_2^- concentrations, a sample aliquot was exposed to O_2 to oxidize Fe(II) rapidly followed by filtration using a syringe filter containing a 0.22 μm mixed cellulose ester membrane. NO_3^- and NO_2^- were quantified by ion chromatography with conductivity detection (Dionex ICS-90 fitted with an AS-4A column; Dionex Corp., Sunnyvale, CA). A mobile phase containing Na_2CO_3 (8 mM) and $NaHCO_3$ (1 mM) was operated at a flow rate of 1 mL min^{-1}. N_2O was quantified by gas chromatography (GC7900, Techcomp, Shanghai) on a packed column [1 m (L) × 3 mm (OD) × 2 mm (ID); 80/100 mesh Porapak] with an electron capture detector. Ferrous iron was quantified photometrically with ferrozine (Lovley and Phillips 1987).

2.4 Stable isotope methods

Headspace N_2O produced from NO_3^- or NO_2^- reduction was dispensed into duplicate gastight serum vials for isotope analysis. $^{15}N/^{14}N$ was quantified by gas chromatography combustion isotope ratio mass spectrometry (GC-IRMS, MAT-253, Finnigan, Bremen, Germany). Experiments were conducted under a He atmosphere in specially fabricated Pyrex media bottles (500 ml) equipped with a vacuum stopcock and crimp-sealed sampling port. N_2O after pre-concentration on line by a PreCon instrument (ThermoFisher Scientific, USA) were processed further in a modified PreCon unit, where H_2O and CO_2 were removed through a long glass tube packed with $MgClO_4$ and NaOH. Then, purified N_2O was introduced into the mass spectrometer for isotope ratio monitoring. The isotopic composition of nitrogenous material is commonly expressed as a delta value:

$$\delta^{15}N = \left(R_{sample}/R_{standard}\text{-}1\right) \times 1000 \quad (1)$$

where R_{sample} and $R_{standard}$ are the $^{15}N/^{14}N$ of the sample and standard, respectively. The standard used for reporting $^{15}N/^{14}N$ ratios is atmospheric N_2 ($^{15}Rair\ N_2 = 0.0036765$) (Jones et al. 2015).

$\delta^{15}N$ of NO_3^- and NO_2^- nitrogen isotopes were determined using azide method (Mcilvin and Altabet 2005). Prior to NO_3^- nitrogen isotope analyses, NO_3^- was reduced to NO_2^- by activated cadmium powder. The NO_2^- was dispensed into duplicate gastight serum vial and purged with N_2 gas, removing any N_2O in the sample produced during the reaction prior to the addition of sodium azide. Finally, the N_2O produced from NO_2^- during the azide step was then analyzed by GC-IRMS.

2.5 Electron microscopy

After 6 days of incubation, the cell-mineral precipitates formed after Fe(II) oxidation were collected for electron microscopy imaging. For scanning electron microscopy (SEM), the precipitates were washed with phosphate buffer (10 mM, pH 7.5) and were fixed with 2.5% glutaraldehyde at 4 °C overnight. The samples were later dehydrated using a series of ethanol dilutions (30, 70, 95, and 100% [twice]) and fixed on cover slips (dried on a molecular sieve) (Klueglein et al. 2014). The cover slips were mounted onto SEM stubs via clear double-sided sticky tape and gold-coated. The samples

Table 1 Experimental setups of the treatments

No.	Treatment	Cells (cells/mL)	NO_3^- (mM)	NO_2^- (mM)	Fe(II) (mM)	Acetate (mM)
1	$Fe(II) + NO_3^-$	–	10	–	5	5
2	$Cell + Fe(II) + NO_3^-$	3.8×10^8	10	–	5	5
3	$Cell + NO_3^-$	3.8×10^8	10	–	–	5
4	Cell + Fe(II)	3.8×10^8	–	–	5	5
5	$Fe(II) + NO_2^-$	–	–	4	5	5
6	$Cell + Fe(II) + NO_2^-$	3.8×10^8	–	4	5	5
7	$Cell + NO_2^-$	3.8×10^8	–	4	–	5

were observed with SEM/EDS (Merlin, Zeiss, Germany) using 5 kV accelerating voltage and at a working distance of 8.7 mm. The EDS spectra provided a primary mineral composition (Zhao et al. 2013).

For transmission electron microscopy (TEM) analyses, the precipitates were fixed for 2 h in 2.5% glutaraldehyde at 4 °C, centrifuged (5000 rpm, 10 min), and rinsed three times in phosphate buffer (10 mM, pH 7.5) for 12 h at 4 °C. The samples were post-fixed for 90 min in 1% OsO_4 in the same buffer, rinsed three times in distilled water, dehydrated in graded ethanol (30, 70, 95, and 100% [once]) and propylene oxide-1,2 and progressively embedded in epoxy resin (Epoxy, Sigma) (Klueglein et al. 2014). Ultrathin sections (40-nm thick) were cut with an ultramicrotome (UCT, Leica, Germany). The ultrathin sections were fixed on copper grids and were observed with TEM (Tecnai 12, FEI, Netherlands) using 80 kV accelerating voltage.

2.6 X-ray diffraction (XRD) analysis

After 6 days of incubation, the Fe(III) precipitates were centrifuged for 15 min at 10,000 rpm and subsequently freeze-dried for 48 h at − 60 °C. Minerals were identified with a Bruker D8 Advance X-ray diffraction instrument (Bruker AXS GmbH, Germany) equipped with a Co KX-ray tube and operating at 40 kV and 40 mA. The MDI Jade 7 software was used for mineral phase identification.

3 Results

3.1 Identification of the strain

The strain designated LS-2 was a gram-negative, facultative anaerobic bacterium. Cells were rod-shaped with a length of 1–2 μm and had monopolar flagella (Fig. 1a). A BLAST analysis of the 16S rRNA gene revealed that strain LS-2 belonged to the *gamma* subclass of Proteobacteria and showed the closest relationship with the denitrifying bacterium *Pseudomonas stutzeri* ATCC 17588^T (AF094748), with a 99.2% similarity (Fig. 1b). Therefore, the strain was identified as *Pseudomonas stutzeri* LS-2 and has been deposited in the China General Microbiological Culture Collection Center (CGMCC 11556). The 16S rRNA sequences of the strain LS-2 were deposited in GenBank under the accession number KY274147.

3.2 Kinetics of Fe(II) oxidation during nitrate reduction

To investigate microbial NO_3^- reduction by *P. stutzeri* LS-2 in the presence of Fe(II), four treatments were carried out (i.e., $Fe(II) + NO_3^-$, $Cell + Fe(II) + NO_3^-$, $Cell + NO_3^-$, and Cell + Fe(II)) (Table 1). Fe(II) was completely oxidized within 3 days in the $Cell + Fe(II) + NO_3^-$ treatment (Fig. 2a) with a rate of Fe(II) oxidation of 1.2 d^{-1} (Table 2). Neither Fe(II) oxidation nor NO_3^- reduction was observed in the treatment of Cell + Fe(II) or $Fe(II) + NO_3^-$. NO_3^- was completely reduced within 2 days in the $Cell + NO_3^-$ treatment, while NO_3^- reduction was slowed down in the $Cell + Fe(II) + NO_3^-$ treatment with only 21% of the NO_3^- reduced at the end of incubation (day 6) (Fig. 2b). The rates of NO_3^- reduction were 3.5 and 0.026 d^{-1} in the treatments of $Cell + NO_3^-$ and $Cell + Fe(II) + NO_3^-$, respectively (Table 2). Most of the NO_3^- consumed was transferred to NO_2^- in which the NO_2^- at the end of incubation was accumulated up to 7.2 mM and 1.9 mM in the treatments of $Cell + NO_3^-$ (72% of the NO_3^- consumed) and $Cell + Fe(II) + NO_3^-$ (85% the NO_3^- consumed), respectively (Fig. 2c). The N_2O concentration increased over time and reached a maximum value of 0.02 mM and 0.04 mM in the $Cell + NO_3^-$ and $Cell + Fe(II) + NO_3^-$ treatments on day 4, respectively (Fig. 2d). The above results suggested that Fe(II) oxidation only occurred in the presence of both bacterial cells and nitrate. NO_3^- could be reduced quickly and completely by *P. stutzeri* LS-2 and the microbial reduction was inhibited by the presence of Fe(II). Fe(II) also facilitated the N_2O production.

3.3 Kinetics of Fe(II) oxidation during nitrite reduction

Three treatments were set up (i.e., $Fe(II) + NO_2^-$, $Cell + Fe(II) + NO_2^-$, and $Cell + NO_2^-$) to investigate the Fe(II)

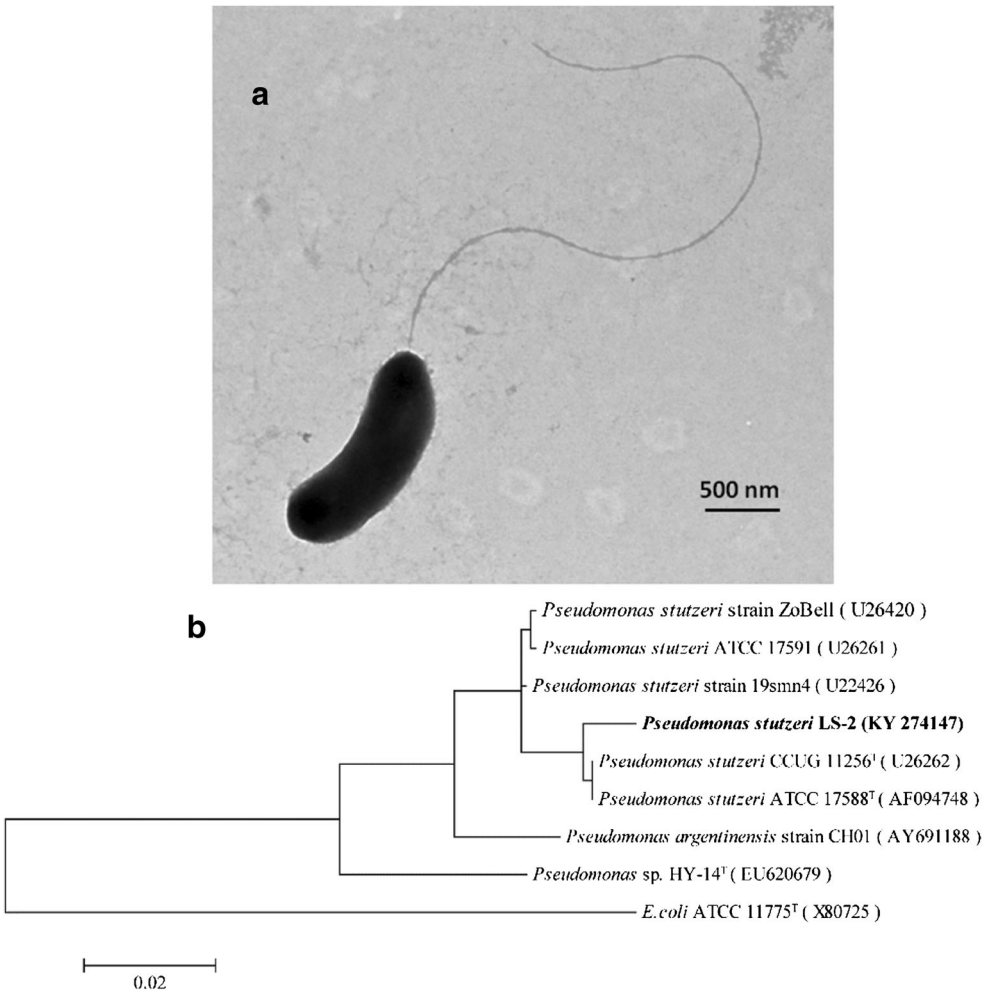

Fig. 1 **a** TEM image of cell of strain *Pseudomonas stutzeri* LS-2 grown anaerobically with 5 mM acetate and 10 mM nitrate (scale bar 500 nm). **b** A neighbor-joining tree based on 16S rRNA sequences shows the phylogenetic affiliation of *P. stutzeri* strain LS-2. Bootstrap values were determined based on 1000 replicates. The numbers in parentheses are the accession numbers. The scale bar represents a 2% sequence difference

oxidation and NO_2^- reduction by *P. stutzeri* LS-2. Similar rates of Fe(II) oxidation were observed in both $Fe(II) + NO_2^-$ (0.32 d^{-1}) and $Cell + Fe(II) + NO_2^-$ (0.31 d^{-1}) treatments (Fig. 3a and Table 2). At the end of incubation, 87−90% of the Fe(II) was oxidized in these two treatments. In the $Cell + NO_2^-$ treatment, NO_2^- was completely reduced at a rate of 1.78 d^{-1} within 2 days (Fig. 3b and Table 2). However, the NO_2^- reduction rate was only 0.13 and 0.15 d^{-1} in the $Fe(II) + NO_2^-$ and $Cell + Fe(II) + NO_2^-$ treatments, respectively (Table 2), in which 53–58% of the NO_2^- were reduced (Fig. 3b). In the $Cell + NO_2^-$ treatment, the concentration of N_2O was 0.03 mM on day 1, and then decreased to 0 mM during days 2–6. The N_2O concentration increased over time in a similar trend in the $Fe(II) + NO_2^-$ and $Cell + Fe(II) + NO_2^-$ treatments, both of which produced 0.15 mM at the end of incubation (Fig. 3c). The above results indicated that the presence of Fe(II) inhibited the NO_2^- reduction by *P. stutzeri* LS-2, but the Fe(II) oxidation and NO_2^- reduction were not affected by the presence of *P. stutzeri* LS-2.

3.4 Stable isotope fractionation of $\delta^{15}N\text{-}N_2O$

The results in Fig. 4 display the changes of $\delta^{15}N\text{-}N_2O$ with time dependence in the treatments with N_2O production during NO_3^- or NO_2^- reduction. The $\delta^{15}N$ values of NO_3^- and NO_2^- supplied in this study are − 0.2 and − 7.3‰, respectively. The values of $\delta^{15}N\text{-}N_2O$ decreased from + 7.8 to − 9.9‰ over time in the microbial treatments of $Cell + NO_2^-$ and $Cell + NO_3^-$. Those values were constant at − 16 ± 0.64 ‰ in the chemical treatment of Fe(II) + NO_2^- during the time course of experiment, which was clearly different from those of the microbial treatments. The $\delta^{15}N\text{-}N_2O$ values in the $Cell + Fe(II) + NO_2^-$ treatment increased gradually from − 23‰ on day 1 to − 18‰ on day 6, which was close to those values of the $Fe(II) + NO_2^-$ treatment. This finding suggested that the N_2O produced from the $Cell + Fe(II) + NO_2^-$ treatment was primarily of chemical origin. In the $Cell + Fe(II) + NO_3^-$ treatment, the $\delta^{15}N\text{-}N_2O$ values increased from − 37‰ on day 1 to − 25‰ on day 6, which was different from those of microbial or chemical treatments.

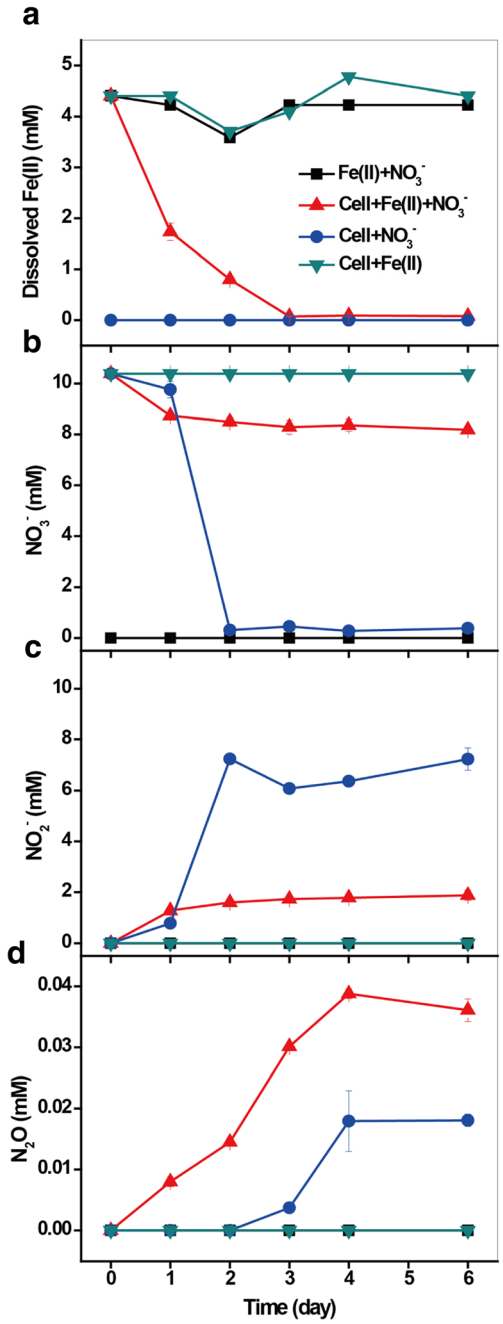

Fig. 2 Concentrations of **a** dissolved Fe(II), **b** NO_3^-, **c** NO_2^-, and **d** N_2O with time dependence in the treatments of Fe(II) + NO_3^-, Cell + Fe(II) + NO_3^-, Cell + NO_3^-, and Cell + Fe(II). Data were presented as the means ± standard deviations (SD) of triplicate

3.5 Fe(III) mineral formation and cell encrustation

Mineral precipitates were only formed in the three treatments with Fe(II) oxidation (i.e., Cell + Fe(II) + NO_3^-, Cell + Fe(II) + NO_2^-, and Fe(II) + NO_2^-), all of which showed regular lath-like structures based on the SEM images in Fig. 5a, b, c. The EDS data indicated the presence of iron and oxygen in the minerals (Table S1, Electronic Supplementary Material). The XRD patterns showed that a classical lepidocrocite (γ-FeOOH) phase

Table 2 The first-order rate constants of Fe(II) oxidation and NO_3^-/NO_2^- reduction in different treatments

No.	Treatment	Fe(II) oxidation		NO_3^-/NO_2^- reduction	
		$k/(d^{-1})$	R^2	$k/(d^{-1})$	R^2
1	Fe(II) + NO_3^-	–	–	–	–
2	Cell + Fe(II) + NO_3^-	1.2 ± 0.081	0.914	0.026 ± 0.080	0.998
3	Cell + NO_3^-	–	–	3.5 ± 0.040	0.992
4	Cell + Fe(II)	–	–	–	–
5	Fe(II) + NO_2^-	0.32 ± 0.020	0.988	0.13 ± 0.014	0.949
6	Cell + Fe(II) + NO_2^-	0.31 ± 0.013	0.994	0.15 ± 0.039	0.742
7	Cell + NO_2^-	–	–	1.8 ± 0.032	0.978

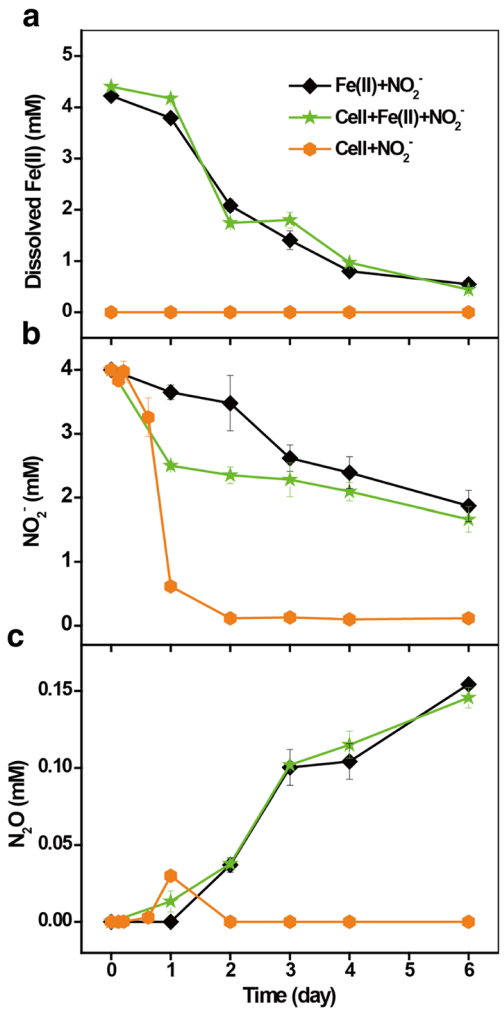

Fig. 3 Concentrations of **a** dissolved Fe(II), **b** NO_2^-, and **c** N_2O with time dependence in the treatments of Fe(II) + NO_2^-, Cell + Fe(II) + NO_2^-, and Cell + NO_2^-. Data were presented as the means ± standard deviations (SD) of triplicate

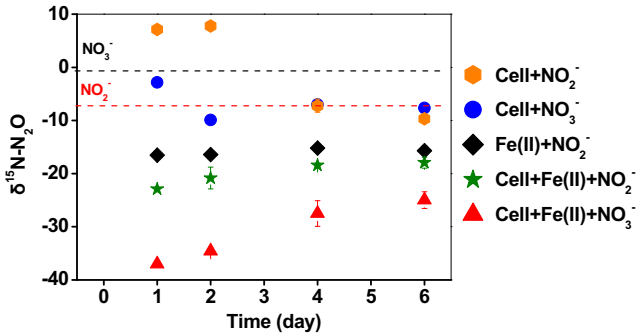

Fig. 4 Evolution of isotopic fractionation $\delta^{15}N$ in N_2O during NO_3^- or NO_2^- reduction in the treatments of Cell + NO_2^-, Cell + NO_3^-, Fe(II) + NO_2^-, Cell + Fe(II) + NO_2^-, and Cell + Fe(II) + NO_3^-. The $\delta^{15}N$ values of NO_3^- and NO_2^- supplied in this study are − 0.2 and − 7.3‰, respectively (dash lines). Data are presented as the means ± standard deviations (SD) of triplicate reactions

was formed in the three treatments (Fig. 5f). The intensities of the characteristic diffraction peaks of γ-FeOOH in the chemical treatment of Fe(II) + NO_2^- were significantly lower than those of the Cell + Fe(II) + NO_3^- and Cell + Fe(II) + NO_2^- treatments, suggesting that the γ-FeOOH formed in the Fe(II) + NO_2^- treatment had a lower level of crystallinity compared with the other two treatments (Fig. 5f). In the Cell + Fe(II) + NO_3^- and Cell + Fe(II) + NO_2^- treatments, the bacterial cells were fully covered by the Fe(III) minerals as indicated by the arrows in Fig. 5a, b. The TEM images of cell-mineral precipitates showed that the cell surface was encrusted with Fe(III) minerals and there was a mineral layer within the periplasm, as well (arrow pointing in Fig. 5d, e).

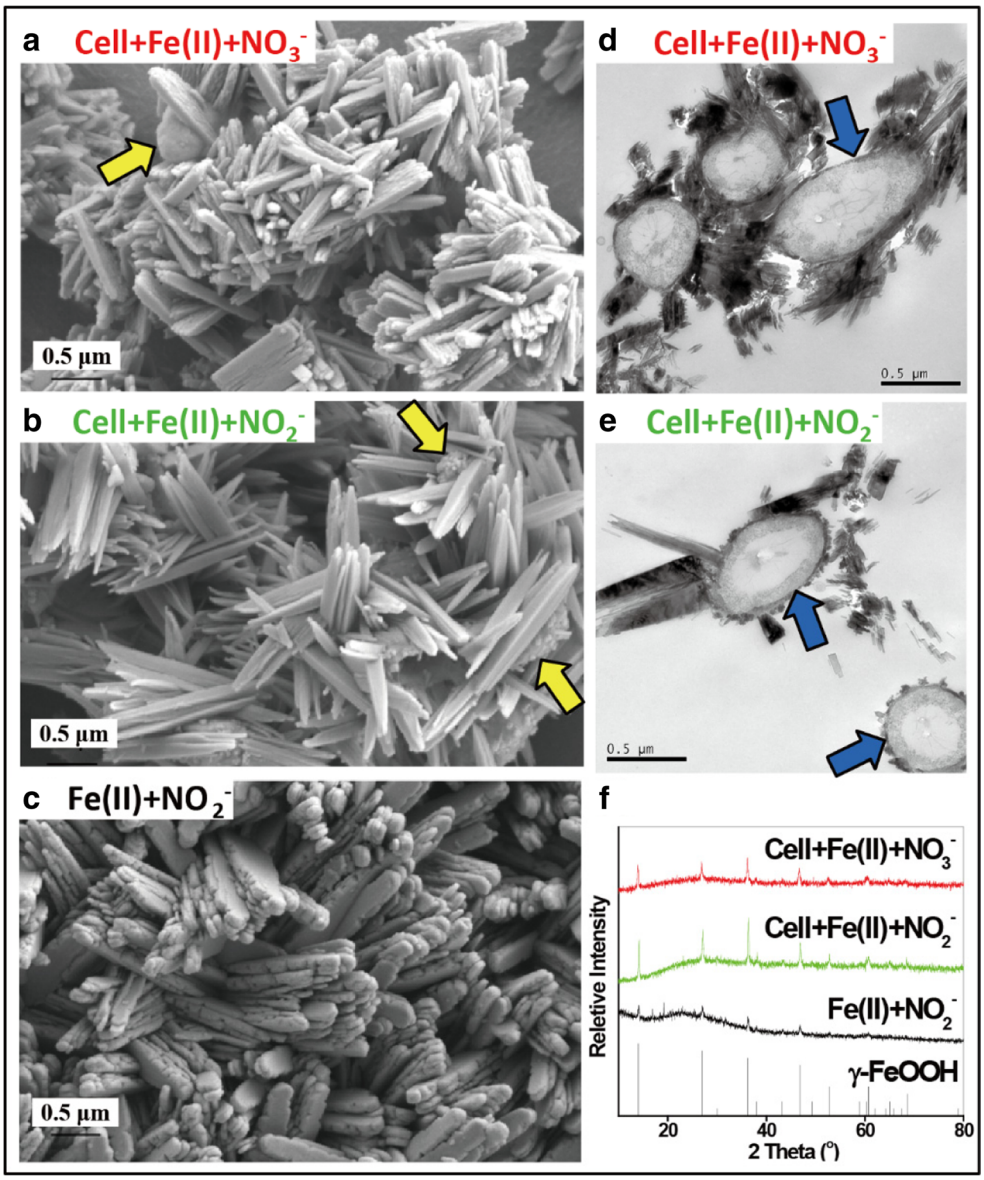

Fig. 5 Scan electron microscopic (SEM) images (**a**–**c**), transmission electron microscopic (TEM) images (**d** and **e**), and X-ray diffraction (XRD) spectra of the Fe mineral precipitates (**f**) from the treatments of Cell + Fe(II) + NO_3^-, Cell + Fe(II) + NO_2^-, and Fe(II) + NO_2^- after 6 days of inoculation. Yellow arrows indicate LS-2 cells were surrounded by minerals, and blue arrows indicate mineral precipitations were observed in the periplasm

4 Discussion

4.1 Effect of Fe(II) oxidation on nitrate reduction by *P. stutzeri* LS-2

P. stutzeri is among the most active denitrifying heterotrophic bacteria and possesses all the enzymes involved in the four successive denitrification pathway steps (Lalucat et al. 2006). After complete NO_3^- reduction by *P. stutzeri* LS-2 in the Cell + NO_3^- treatment, 72 and 0.2% of the NO_3^- consumed was determined to be NO_2^- and N_2O, respectively. NO_2^- accumulation is a widespread phenomenon observed during the denitrification process mediated by *P. stutzeri*, which is considered to be the result of an unbalanced NO_3^- and NO_2^- reduction (Xu and Enfors 1996). In previous studies regarding Fe(II) oxidation coupled to NO_3^- reduction by denitrifying bacteria, complete NO_3^- reduction was observed by *P. denitrificans* strain ATCC19367 or strain Pd 1222 (Klueglein et al. 2014), while only 17–21% of the added NO_3^- was consumed by *P. stutzeri* ATCC 17588 or *P. denitrificans* ATCC 17741 (Muehe et al. 2009). In this study, the presence of Fe(II) resulted in an inhibition on NO_3^- reduction by *P. stutzeri* LS-2 (Fig. 2b), indicating that Fe(II) oxidation may restrain nitrate reductase activity or block NO_3^- reduction. Accumulation of NO_2^- was up to 85% in the Cell + Fe(II) + NO_3^- treatment (Fig. 2c), which was suggested to be a result of encrustation of the nitrite reductase in the periplasm (Klueglein and Kappler 2013). However, there was no NO_2^- accumulation during the nitrate reduction and Fe(II) oxidation by *P. stutzeri* ATCC 17588 or *P. denitrificans* ATCC 17741 (Muehe et al. 2009). The effect of Fe(II) oxidation on NO_3^- reduction and NO_2^- accumulation by denitrifying bacteria appears to vary on a case by case basis.

N_2O is commonly produced during chemodenitrification as well as Fe(II) oxidation and nitrate reduction by denitrifying bacteria (Muehe et al. 2009; Jones et al. 2015). The Fe(II) oxidation strongly affects the N_2O emission via donating electrons to denitrification in paddy soils (Wang et al. 2016). The $\delta^{15}N$-N_2O values on the first day varied among different treatments (Fig. 4), which may be due to the difference in N transformation. In Cell + NO_2^- treatment, 85% of the NO_2^- added was consumed on day 1, with only 0.03 mM of N_2O formed. Based on N mass balance considerations, about 3.4 mM of the reduced NO_2^- was transformed as NO and/or N_2. Generally, ^{14}N reacts more quickly relative to ^{15}N (Barford et al. 1999). Hence, it is speculated that N_2 was the dominant product from NO_2^- reduction in Cell + NO_2^- treatment, resulting in relatively high $\delta^{15}N$ accumulation in N_2O. Meanwhile, in Cell + NO_3^- treatment, only 6% of the NO_3^- added was consumed and 90% of the consumed NO_3^- was present as NO_2^-, with no formation of N_2O and only 0.1 mM of NO/N_2. Its $\delta^{15}N$-N_2O value is close to that of $\delta^{15}N$ in NO_3^-, which is probably due to the fact that most of the N is present as NO_3^- and the yield of N intermediates was limited. The concentration of N_2O was less than 0.02 mM on day 1 in Fe(II) + NO_2^-, Cell + Fe(II) + NO_2^-, and Cell + Fe(II) + NO_3^- treatments, resulting in 0.3 mM, 1.4 mM, and 0.4 mM transferred as NO/N_2, respectively. It is reported that NO is a heavy pool of N accumulation and ^{14}N is preferentially reacted to N_2O (Toyoda et al. 2005; Jones et al. 2015). Accordingly, the relatively low $\delta^{15}N$ accumulation in N_2O in these three treatments suggests that NO is likely the dominant product at this time interval.

The $\delta^{15}N$-N_2O in the two microbial treatments (i.e., Cell + NO_3^- and Cell + NO_2^-) decreased since day 1–2, which is possibly attributed to that the NO_3^-/NO_2^- added was completely reduced and further N transformation was ceased, resulting in a balanced $\delta^{15}N$-N_2O value close to that of $\delta^{15}N$ in NO_2^- during the rest of incubation. The $\delta^{15}N$-N_2O in our chemical treatment of Fe(II) + NO_2^- (-16 ± 0.64 ‰) is within the wide range of $\delta^{15}N$-N_2O during the chemodenitrification (-16.8 to 0.2‰) as reported previously (Jones et al. 2015). The analogous reaction rates of NO_2^- reduction and Fe(II) oxidation (Table 2), in combination with the similar values of $\delta^{15}N$-N_2O (Fig. 4) between the Fe(II) + NO_2^- and Cell + Fe(II) + NO_2^- treatments, indicated that the N_2O produced during NO_2^- reduction and Fe(II) oxidation in the presence of cells was mainly due to the chemodenitrification process between NO_2^- and Fe(II). Similarly, the N_2O produced from the NO_3^- reduction by *Shewanella putrefaciens* in the presence of iron oxide is primarily of chemical origin per the stable isotope studies of $\delta^{15}N$ in N_2O (Cooper et al. 2003). The slight increase in $\delta^{15}N$-N_2O of Cell + Fe(II) + NO_2^- treatment may be caused by a further reduction from N_2O to N_2 in which ^{14}N is preferentially reacted (Barford et al. 1999).

In the Cell + Fe(II) + NO_3^- treatment, the presence of Fe(II) facilitated N_2O production during denitrification by *P. stutzeri* LS-2 (Fig. 2d), and its $\delta^{15}N$-N_2O values were different from those of microbial or chemical treatments (Fig. 4). Previous study blocks the N_2O reduction process using an acetylene inhibition technique and observes negative $\delta^{15}N$-N_2O values (from -37 to -29‰) during denitrification (Toyoda et al. 2005). Fe(III) precipitation occurred in the periplasm (Fig. 5d), by which both periplasimc NO_2^- and N_2O reductases can be easily coated and inactivated (Kappler et al. 2005; Carlson et al. 2013), resulting in accumulation of NO_2^- and N_2O (Fig. 2c, d). As such, the increase in N_2O in the Cell + Fe(II) + NO_3^- treatment should be from NO reduction which can be mediated via the cytoplasmic-membrane bound NO reductase and chemodenitrification. If this is the case that N_2O reduction is blocked by the Fe(III) precipitation, similar negative $\delta^{15}N$-N_2O could be obtained as well, and further N_2O formation from NO with highly accumulated ^{15}N could also lead to an increase in $\delta^{15}N$-N_2O in some extent.

4.2 Effect of nitrate reduction on Fe(II) oxidation by *P. stutzeri* LS-2

The added Fe(II) was completely oxidized within 3 days during the denitrification by *P. stutzeri* LS-2 (Fig. 2a). Similarly, complete Fe(II) oxidation has also been reported during NO_3^- reduction by the denitrifier *Paracoccus denitrificans* (Klueglein et al. 2014), while incomplete Fe(II) oxidation was observed in the nitrate-reducing Fe(II) oxidation culture of other denitrifiers such as *Pseudomonas stutzeri*, *Nocardioides* sp., and *Rhodanobacter* sp. (Muehe et al. 2009; Nordhoff et al. 2017). Such a discrepancy may be associated with a difference in bacterial species, cell metabolic states, Fe(II) and NO_3^- initial concentrations, and incubation medium compositions used in different studies, which also leads to a difference in Fe(III) mineralization and cell encrustation (Larese-Casanova et al. 2010; Nordhoff et al. 2017).

Several studies have reported nitrate-reducing Fe(II) oxidation in pure *Pseudomonas* sp. culture (Muehe et al. 2009; Su et al. 2015; Zhang et al. 2015); however, few studies characterize the iron mineralization after Fe(II) oxidation. Lepidocrocite formation appears to be favorable in a buffer without any iron-complexing anions such as MOPS buffer (Larese-Casanova et al. 2010), while goethite is the primary Fe(III) phase formed in a carbonate buffer even with the same bacterial strain (Klueglein et al. 2014; Senko et al. 2005). This result can explain the formation of lepidocrocite in this study since all the experiments were carried out in the PIPES buffer without any iron-complexing anions. It has been demonstrated that the Fe(III) mineralogy is mainly controlled by the geochemical condition of the solution but not the mode of Fe(II) oxidation (biotic or abiotic) (Larese-Casanova et al. 2010). These results support our finding that lepidocrocite was formed in all the treatments with Fe(II) oxidation occurring in the same medium (Fig. 5f). Treatments of Cell + Fe(II) + NO_3^- and Cell + Fe(II) + NO_2^- showed relatively higher crystallinity of lepidocrocite than Fe(II) + NO_2^-, indicated that the presence of *P. stutzeri* LS-2 probably favors the formation of highly crystalline Fe(III) minerals.

The chemodenitrification reactions between Fe(II) and NO_2^- in a PIPES buffer can generate a variety of Fe(III) (hydr)oxide minerals including ferrihydrite, lepidocrocite and goethite (Jones et al. 2015). The experiment with equimolar concentrations of Fe(II) and NO_2^- results in a nearly equal proportion of the three Fe(III) minerals after 2 days of reaction (Jones et al. 2015). Only lepidocrocite was detected after a 6-day incubation in our chemical treatment of Fe(II) + NO_2^- with initial concentrations of Fe(II) and NO_2^- of 5 and 4 mM, respectively (Table 1). This result may be caused by the difference in the composition of reaction solution and the reaction time.

Fe(II) oxidation in the presence of denitrifying bacteria is considered to be driven by the intermediates (mainly NO_2^-) produced during denitrification (Muehe et al. 2009; Klueglein et al. 2014; Nordhoff et al. 2017); this is because accumulation of NO_2^- in these cultures is commonly observed (Fig. 2) and the chemodenitrification reaction is rapid even without catalysts (Fig. 3) (Klueglein and Kappler 2013; Jones et al. 2015). The chemical oxidation of Fe(II) by NO_2^- in denitrifying bacterial culture does not allow control over the location of Fe(III) precipitation and even occurs in the periplasm where the NO_2^- was formed after NO_3^- reduction (Lalucat et al. 2006; Miot et al. 2009; Nordhoff et al. 2017). The cell encrustation on the cell surfaces and in the periplasm in

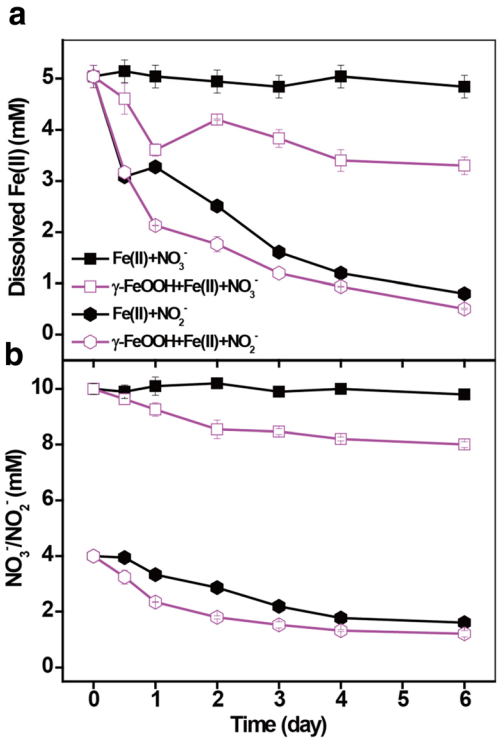

Fig. 6 Concentrations of **a** dissolved Fe(II), and **b** NO_3^- or NO_2^- with time dependence in the treatments of Fe(II) + NO_3^-, γ-FeOOH + Fe(II) + NO_3^-, Fe(II) + NO_2^-, and γ-FeOOH + Fe(II) + NO_2^-. The initial concentration of γ-FeOOH was 5 mM. Data are presented as the means ± standard deviations (SD) of triplicate reactions

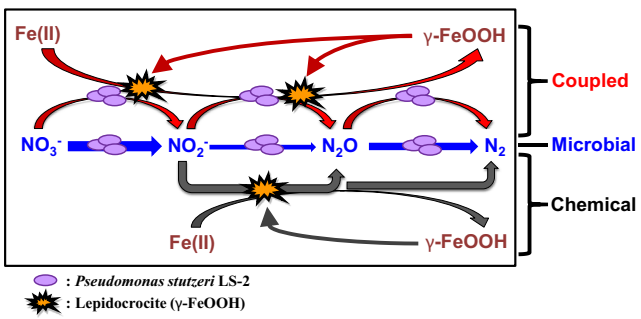

Fig. 7 The coupled interaction between denitrification and Fe(II) oxidation mediated by *Pseudomonas stutzeri* LS-2 included microbial and chemical processes

the Cell + Fe(II) + NO_3^- treatment (Fig. 5d, e) suggested that chemodenitrification contributed to the Fe(II) oxidation. Because of encrustation, the mineral coatings on the cell surface may hinder NO_3^- transport and nutrient uptake into the cell and may eventually result in inhibition of cell growth (Klueglein et al. 2014). This can be supported by the substantially lower concentrations of cell protein observed in Cell + Fe(II) + NO_3^- and Cell + Fe(II) + NO_2^- treatments, relative to those of Cell + NO_3^- and Cell + NO_2^- treatments (Fig. S1, Electronic Supplementary Material).

The presence of a mineral surface has a catalytic effect on Fe(II) oxidation by NO_3^-/NO_2^- (Sørensen and Thorling 1991; Tai and Dempsey 2009). Supplementary experiments were conducted with Fe(II) and NO_3^-/NO_2^- in the absence and presence of lepidocrocite. The kinetics results indicated that the presence of lepidocrocite did accelerate the reactions between Fe(II) and NO_3^-/NO_2^- (Fig. 6, and Table S2 in the Electronic Supplementary Material), which is consistent with previous study showing the accelerated effect of goethite on Fe(II) oxidation by NO_2^- (Klueglein and Kappler 2013). Hence, the formation of lepidocrocite in this study can contribute to the Fe(II) oxidation during the denitrification by *P. stutzeri* LS-2. In summary, the Fe(II) oxidation and nitrate reduction mediated by *P. stutzeri* LS-2 included both microbial and chemical processes, as presented in the Fig. 7.

5 Conclusions

The present study observed that the denitrifying bacterium *P. stutzeri* LS-2, isolated from paddy soil in southern China, could rapidly reduce NO_3^- or NO_2^- in the absence of Fe(II). The addition of Fe(II) slowed the microbial NO_3^- or NO_2^- reduction, which was probably due to encrustation on the cell surface and in the periplasm. The NO_2^- produced during NO_3^- reduction by *P. stutzeri* LS-2 primarily reacted chemically with Fe(II). Fe(II) oxidation during denitrification by *P. stutzeri* LS-2 resulted in the formation of lepidocrocite, which further accelerated the chemical reactions between Fe(II) and NO_3^-/NO_2^-. Our findings suggested that stable isotope fractionations of δ^{15}N-N_2O in combination with the transformation kinetics of iron and nitrogen are helpful approaches to distinguish the chemical and biological reactions involved in Fe(II) oxidation and nitrate reduction by denitrifying bacteria.

Funding information This work was funded by the National Natural Science Foundations of China (41330857 and 41571130052), the Guangdong Natural Science Funds for Distinguished Young Scholars (2017A030306010), the Australian Research Council DECRA grant (DE150100500) and the SPICC Program (Scientific Platform and Innovation Capability Construction Program of GDAS).

References

Barford CC, Montoya JP, Altabet MA, Mitchell R (1999) Steady-state nitrogen isotope effects of N_2 and N_2O production in *Paracoccus denitrificans*. Appl Environ Microbiol 65(3):989–994

Bruce RA, Achenbach LA, Coates JD (1999) Reduction of (per)chlorate by a novel organism isolated from paper mill waste. Environ Microbiol 1(4):319–329. https://doi.org/10.1046/j.1462-2920.1999.00042.x

Byrne-bailey KG, Weber KA, Chair AH, Bose S, Knox T, Spanbauer TL, Chertkov O, Coates JD (2010) Completed genome sequence of the anaerobic iron-oxidizing bacterium *Acidovorax ebreus* strain TPSY. J Bacteriol 192(5):1475–1476. https://doi.org/10.1128/JB.01449-09

Carlson HK, Clark IC, Blazewicz SJ, Iavarone AT, Coates JD (2013) Fe(II) oxidation is an innate capability of nitrate-reducing bacteria that involves abiotic and biotic reactions. J Bacteriol 195(14):3260–3268. https://doi.org/10.1128/JB.00058-13

Chakraborty A, Roden EE, Schieber J, Picardal F (2011) Enhanced growth of *Acidovorax* sp. strain 2AN during nitrate-dependent Fe(II) oxidation in batch and continuous-flow systems. Appl Environ Microbiol 77(24):8548–8556. https://doi.org/10.1128/AEM.06214-11

Chaudhuri SK, Lack JG, Coates JD (2001) Biogenic magnetite formation through anaerobic biooxidation of Fe(II). Appl Environ Microbiol 67(6):2844–2848. https://doi.org/10.1128/AEM.67.6.2844-2848.2001

Cooper DC, Picardal FW, Schimmelmann A, Coby AJ (2003) Chemical and biological interactions during nitrate and goethite reduction by *Shewanella putrefaciens* 200. Appl Environ Microbiol 69(6):3517–3525. https://doi.org/10.1128/AEM.69.6.3517-3525.2003

Delong EF (1992) Archaea in coastal marine environments. Proc Nat Acad Sci US 89(12):5685–5689. https://doi.org/10.1073/pnas.89.12.5685

Heil J, Wolf B, Brüggemann N, Emmenegger L, Tuzson B, Vereecken H, Mohn J (2014) Site-specific ^{15}N isotopic signatures of abiotically produced N_2O. Geochim Cosmochim Acta 139:72–82. https://doi.org/10.1016/j.gca.2014.04.037

Jones LC, Peters B, Pacheco JS, Lezama, Casciotti KL, Scott F (2015) Stable isotopes and iron oxide mineral products as markers of chemodenitrification. Environ Sci Technol 49(6):3444–3452. https://doi.org/10.1021/es504862x

Kappler A, Pasquero C, Konhauser KO, Newman DK (2005) Deposition of banded iron formations by anoxygenic phototrophic Fe(II)-oxidizing bacteria. Geology 33(11):865–868. https://doi.org/10.1130/G21658.1

Klueglein N, Kappler A (2013) Abiotic oxidation of Fe(II) by reactive nitrogen species in cultures of the nitrate-reducing Fe(II) oxidizer *Acidovorax* sp. BoFeN1 - questioning the existence of enzymatic Fe(II) oxidation. Geobiology 11(2):180–190. https://doi.org/10.1111/gbi.12019

Klueglein N, Zeitvogel F, Stierhof YD, Floetenmeyer M, Konhauser KO, Kappler A, Obst M (2014) Potential role of nitrite for abiotic Fe(II) oxidation and cell encrustation during nitrate reduction by denitrifying bacteria. Appl Environ Microbiol 80(3):1051–1061. https://doi.org/10.1128/AEM.03277-13

Lack JG, Chaudhuri SK, Chakraborty R, Achenbach LA, Coates JD (2002) Anaerobic biooxidation of Fe(II) by *Dechlorosoma suillum*. Microb Ecol 43(4):424–431. https://doi.org/10.1007/s00248-001-1061-1

Lalucat J, Bennasar A, Bosch R, García-Valdés E, Palleroni NJ (2006) Biology of *Pseudomonas stutzeri*. Microbiol Mol Biol Rev 70(2):510–547. https://doi.org/10.1128/MMBR.00047-05

Larese-Casanova P, Haderlein SB, Kappler A (2010) Biomineralization of lepidocrocite and goethite by nitrate-reducing Fe(II)-oxidizing bacteria: effect of pH, bicarbonate, phosphate, and humic acids.

Geochim Cosmochim Acta 74(13):3721–3734. https://doi.org/10.1016/j.gca.2010.03.037

Laufer K, Nordhoff M, Røy H, Schmidt C, Behrens S, Jørgensen BB, Kappler A (2015) Coexistence of microaerophilic, nitrate-reducing, and phototrophic Fe(II) oxidizers and Fe(III) reducers in coastal marine sediment. Appl Environ Microbiol 82(5):1433–1447. https://doi.org/10.1128/AEM.03527-15

Li X, Zhang W, Liu T, Chen L, Chen P, Li F (2016) Changes in the composition and diversity of microbial communities during anaerobic nitrate reduction and Fe(II) oxidation at circumneutral pH in paddy soil. Soil Biol Biochem 94:70–79. https://doi.org/10.1016/j.soilbio.2015.11.013

Lovley DR, Phillips EJ (1987) Rapid assay for microbially reducible ferric iron in aquatic sediments. Appl Environ Microbiol 53(7):1536–1540

Mcilvin MR, Altabet MA (2005) Chemical conversion of nitrate and nitrite to nitrous oxide for nitrogen and oxygen isotopic analysis in freshwater and seawater. Anal Chem 77(17):5589–5595. https://doi.org/10.1021/ac050528s

Mejia J, Roden EE, Ginder-vogel MA (2016) Influence of oxygen and nitrate on Fe (hydr)oxide mineral transformation and soil microbial communities during redox cycling. Environ Sci Technol 50(7):3580–3588. https://doi.org/10.1021/acs.est.5b05519

Melton ED, Swanner ED, Behrens S, Schmidt C, Kappler A (2014) The interplay of microbially mediated and abiotic reactions in the biogeochemical Fe cycle. Nat Rev Microbiol 12(12):797–808. https://doi.org/10.1038/nrmicro3347

Miot J, Benzerara K, Morin G, Bernard S, Beyssac O, Larquet E, Kappler A, Guyot F (2009) Transformation of vivianite by anaerobic nitrate-reducing iron-oxidizing bacteria. Geobiology 7(3):373–384. https://doi.org/10.1111/j.1472-4669.2009.00203.x

Muehe EM, Gerhardt S, Schink B, Kappler A (2009) Ecophysiology and the energetic benefit of mixotrophic Fe(II) oxidation by various strains of nitrate-reducing bacteria. FEMS Microbiol Ecol 70(3):335–343. https://doi.org/10.1111/j.1574-6941.2009.00755.x

Nordhoff M, Tominski C, Halama M, Byrne JM, Obst M, Kleindienst S, Behrens S, Kappler A (2017) Insights into nitrate-reducing Fe(II) oxidation mechanisms by analyzing cell-mineral associations, cell encrustation and mineralogy in the chemolithoautotrophic enrichment culture KS. Appl Environ Microbiol 83(13):e00752–e00717. https://doi.org/10.1128/AEM.00752-17

Senko JM, Dewers TA, Krumholz LR (2005) Effect of oxidation rate and Fe(II) state on microbial nitrate-dependent Fe(III) mineral formation. Appl Environ Microbiol 71(11):7172–7177. https://doi.org/10.1128/AEM.71.11.7172-7177.2005

Sørensen J, Thorling L (1991) Stimulation by lepidocrocite (γ-FeOOH) of Fe(II)-dependent nitrite reduction. Geochim Cosmochim Acta 55(5):1289–1294. https://doi.org/10.1016/0016-7037(91)90307-Q

Straub KL, Buchholz-cleven BE (1998) Enumeration and detection of anaerobic ferrous iron-oxidizing, nitrate-reducing bacteria from diverse European sediments. Appl Environ Microbiol 64(12):4846–4856

Straub KL, Benz M, Schink B, Widdel F (1996) Anaerobic, nitrate-dependent microbial oxidation of ferrous iron. Appl Environ Microbiol 62(4):1458–1460

Su JF, Shao SC, Huang TL, Ma F, Yang SF, Zhou ZM, Zheng SC (2015) Anaerobic nitrate-dependent iron(II) oxidation by a novel autotrophic bacterium, *Pseudomonas* sp. SZF15. J Environ Chem Eng 3(3):2187–2193. https://doi.org/10.1016/j.jece.2015.07.030

Sutka RL, Ostrom NE, Ostrom PH, Breznak JA, Gandhi H, Pitt AJ, Li F (2006) Distinguishing nitrous oxide production from nitrification and denitrification on the basis of isotopomer abundances. Appl Environ Microbiol 72(1):638–644. https://doi.org/10.1128/AEM.72.1.638-644.2006

Tai YL, Dempsey BA (2009) Nitrite reduction with hydrous ferric oxide and Fe(II): stoichiometry, rate, and mechanism. Water Res 43(2):546–552. https://doi.org/10.1016/j.watres.2008.10.055

Toyoda S, Mutobe H, Yamagishi H, Yoshida N, Tanji Y (2005) Fractionation of N_2O isotopomers during production by denitrifier. Soil Biol Biochem 37(8):1535–1545. https://doi.org/10.1016/j.soilbio.2005.01.009

Wang M, Hu R, Zhao J, Kuzyakov Y, Liu S (2016) Iron oxidation affects nitrous oxide emissions via donating electrons to denitrification in paddy soils. Geoderma 271:173–180. https://doi.org/10.1016/j.geoderma.2016.02.022

Weber KA, Achenbach LA, Coates JD (2006) Microorganisms pumping iron: anaerobic microbial iron oxidation and reduction. Nat Rev Microbiol 4(10):752–764. https://doi.org/10.1038/nrmicro1490

Wunderlin P, Mohn J, Joss A, Emmenegger L, Siegrist H (2012) Mechanisms of N_2O production in biological wastewater treatment under nitrifying and denitrifying conditions. Water Res 46(4):1027–1037. https://doi.org/10.1016/j.watres.2011.11.080

Xu B, Enfors SO (1996) Modeling of nitrite accumulation by the denitrifying bacterium *Pseudomonas stutzeri*. J Ferment Bioeng 82(1):56–60. https://doi.org/10.1016/0922-338X(96)89455-4

Yu HY, Wang X, Li F, Li B, Liu C, Wang Q, Lei J (2017) Arsenic mobility and bioavailability in paddy soil under iron compound amendments at different growth stages of rice. Environ Pollut 224:136–147. https://doi.org/10.1016/j.envpol.2017.01.072

Zhang J, Zhou W, Liu B, He J, Shen Q, Zhao FJ (2015) Anaerobic arsenite oxidation by an autotrophic arsenite-oxidizing bacterium from an arsenic-contaminated paddy soil. Environ Sci Technol 49(10):5956–5964. https://doi.org/10.1021/es506097c

Zhao L, Dong H, Kukkadapu R, Agrawal A, Liu D, Zhang J, Edelmann RE (2013) Biological oxidation of Fe(II) in reduced nontronite coupled with nitrate reduction by *Pseudogulbenkiania* sp. strain 2002. Geochim Cosmochim Acta 119:231–247. https://doi.org/10.1016/j.gca.2013.05.033

Zumft WG (1997) Cell biology and molecular basis of denitrification. Microbiol Mol Biol Rev 61(4):533–616